The Influence of Gait Phase on Predicting Lower-Limb Joint Angles

Article *in* IEEE Transactions on Medical Robotics and Bionics · May 2023

DOI: 10.1109/TMRB.2023.3260261

This article has been accepted for publication in IEEE Transactions on Medical Robotics and Bionics. This is the author's version which has not been fully edited and content may change prior to final publication. Citation information: DOI 10.1109/TMRB.2023.3260261

The Influence of Gait Phase on Predicting Lower-limb Joint Angles

David Hollinger
Dept. of Mechanical Engineering
Auburn, AL, USA
dzh0063@auburn.edu

Mark Schall, Jr.
Dept. of Industrial & Sys. Engineering
Auburn, AL, USA
mcs0084@auburn.edu

Howard Chen
Industrial & Systems Engineering & Engineering Management
University of Alabama, Hunstville
hc0060@uah.edu

Sarah Bass
Dept. of Mechanical Engineering
Auburn, AL, USA
smb0186@auburn.edu

Michael Zabala
Dept. of Mechanical Engineering
Auburn, AL, USA
zabalme@auburn.edu

Abstract—Machine learning has seen a rapid increase in applications that harness wearable signals to improve human mobility. Previous work has used machine learning predictors as a means of continuously estimating locomotor intent. Although previous studies perform gait phase classification and joint-level angular prediction, there are currently no studies that compare joint-level prediction performance at various phases of gait. As such, the purpose of this offline study was to analyze how machine learning and deep learning models perform at predicting future joint angles during various phases of gait. EMG, IMU, and joint kinematics collected during level-ground walking from thirty participants and data was separated into six distinct gait phases. Random forest, long short-term memory (LSTM), and bidirectional LSTM was used to predict lower-limb joint angles during the phases of gait. Results indicate that bidirectional LSTM is the most robust performer across the gait cycle, with a mean prediction RMSE of 1.42-5.71 degrees. Our study shows how deep learning methods, such as bidirectional LSTM, can accurately estimate joint angles throughout the gait cycle. Furthermore, we propose future work of deploying models which accurately predict future joint angles throughout the gait cycle for users to sufficiently operate a wearable exoskeleton during locomotion.

Index Terms—Gait phase estimator, joint angle prediction, machine learning, deep learning

I. Introduction

Human intent recognition is often used to sense the user's desired movement. Human intent recognition is beneficial because it can monitor and analyze human behavior, detect abnormalities, and offer feedback to enhance exercise routines. Despite physical activity guidelines recommending adults to participate in at least 150 minutes of moderate to strenuous activity per week, approximately 46.9% of U.S. adults were sufficiently active to experience meaningful health benefits [1]. Walking is one of the most common forms of exercise and is associated with many health benefits, such as lower blood pressure, risk of diabetes and cardiovascular disease [2]. Personalizing a wearable device to a user's gait can increase user engagement and encourage habits of daily walking. Smartphones and smart watches are often used to track physical activity. One way to encourage walking among the general population is through wearable robotic assistance [3].

For healthy individuals, augmentation devices can enhance task capabilities for army soldiers, firefighters, and industrial workers [4]. Mudie et al. [5] argued that military leaders have not yet adopted augmentation wearables for operational use due to their inability to synchronously adapt to the user, task, and environment. Due to the complexity of human movement, users are presented with the challenge of operating wearable devices that move in unison with the user's intended motion.

Hierarchical control architecture for wearable robotics comprises of high-level, mid-level, and low-level controllers [4]. The high-level controller is often used to estimate locomotor intent [6]. Numerous studies have explored high-level controllers for human locomotion such as activity mode classification [7], gait phase estimation [8], walking speed [8], acceleration, and environmental features [13]–[15]. However, high-level controllers may not be able to respond in unison to the user's desired intent when transitioning to a new task or environmental condition (e.g. terrain, slopes, stairs).

One method of estimating movement intent is through control parameter determination, or mid-level control. Mid-level control serves as an intermediate between high-level control and low-level control. Examples of mid-level control are position, velocity, torque [16]–[19], impedance, or admittance control to estimate the user's state within the gait cycle [6]. Additionally, human-in-the-loop optimization is a method for rapid exploration of estimating control parameters and is useful for mid-level controllers [20]. Model-free approaches use reinforcement learning for state-based policy generation [21] and end-to-end learning [22]. Joint angle estimation is used for mid-level control and model-free methods and is crucial for matching lower-limb assistive devices to a user's desired joint angles during locomotion [23].

Although several studies have introduced machine learning algorithms to improve joint kinematic predictions [24], to the knowledge of the authors no studies report the model performance results for joint-level prediction during specific phase windows of gait. One key aspect of locomotion

evaluation missing in these machine learning studies is reporting prediction performance relevant to the gait cycle. Since the phases of gait provide meaningful information on user intent during ambulation, it is worth exploring how joint-level predictors perform at key phases of gait. Previous studies using machine learning to predict joint angles report prediction accuracy for the entire gait cycle [9], [25]. Ng and Chizek, 1997 applied a fuzzy system classifier to predict the gait phase and reported classification accuracy during weight acceptance, midstance, terminal stance, early swing, and late swing [12]. However, it is argued that high-level controllers which classify gait phase, require predefined dynamic models which may not accurately define movement intent compared to machine learning models which uses wearable signals to predict joint kinematics [6]. This is because high-level control generates a sequence of values (e.g., torque profile for one stride) for a given locomotion mode (e.g., walking, running, stair ascent/descent). Conversely, a machine learning-based approach using direct volitional control generates continuous point-by-point updates, which better resembles the user's underlying neuromuscular intent. Therefore, a model-free method, such as machine learning or deep learning, may be more adaptable to the user's intent than high-level controllers [26]–[28]. Furthermore, the lack of prediction comparisons at key movement points (e.g., toe-off phase) can have less than ideal outcomes. For example, peaks in prediction errors at crucial points of the gait cycle may impair one's ability to control an exoskeleton to a desired joint angle [20], delay assistance, and misrepresent the user's desired motion intent during ambulation [29]. These can result in undesirable exoskeleton torque assistance and increased metabolic cost [20]. Deep learning has shown promise in modeling nonlinear sequence-to-sequence problems, such as mapping an input sequence of sensor signals to a kinematic sequence [30]. Walking is considered a dynamic process whereby the current state is dependent on the previous one. Therefore, sequence learning models are useful for locomotor intent by predicting a sequence of kinematics and kinetics [25]. EMG is also advantageous for predicting motion intent because signals can be read approximately 20-200 ms prior to muscle action [31], [32]. Additionally, real-time controllers using EMG signals as inputs have optimal performance when delays are between 100 ms and 125 ms [33]. Delays above the optimal range reduce functional performance and delays above 300 ms are considered unacceptable for real-time applications [34]. Conventional controllers use EMG and IMU signals to predict joint angles across the gait cycle. However, since segment orientations and EMG signals alter throughout a gait cycle, a gait phase-dependent pattern recognition estimator may help maximize the effectiveness of exoskeleton assistance to a user. Furthermore, a machine learning-based predictor should have low prediction errors at critical points of the gait cycle, such as before the toe-off phase.

Here, we tested one machine learning model (Random Forest) and two deep learning models (long short-term memory (LSTM) and bidirectional LSTM) for predicting future lower-limb joint angles. Afterward, we compared the prediction performance at four phases of gait. Although LSTMs are designed to overcome the limitations of standard recurrent neural networks (RNNs), they may not be ideal for predicting all sequence problems. For example, a simpler model using multilayer perceptron or random forest may be more appropriate for sequence problems where the most recent events contain enough relevant information for predicting the next event [28]. LSTM has been shown to perform well for time-series applications [35], However, it is unclear what effect adding a bidirectional layer to the input data would have on predicting future joint angles. As a result, we compared the performance of predicting joint angles using a Random Forest, LSTM, and Bidirectional LSTM (BiLSTM).

Although Ma et al. 2020 and Mundt et al., 2020 used LSTM to predict knee flexion angle with an RMSE of 3.4726 degrees [36] and knee and hip flexion angles with a normalized RMSE of 11.85% and 9.83%, respectively [25], the results were reported for the entire gait cycle. We, therefore, predicted lower limb joint angles using the LSTM model, but evaluated prediction performance during distinct gait phases as opposed to the entire gait cycle.

Therefore, the overall objective of this study was to test several machine learning and deep learning models for predicting lower limb joint angles at 100 ms in the future. Since several studies have found muscle activity to precede limb motion by about 100 ms [31], [32], we selected this prediction time as a method for intent recognition that could potentially be used for naturalistic locomotor intent recognition. We propose a novel way to represent locomotor intent among healthy individuals by comparing model performance during relevant phase windows of the gait cycle.

This offline study explores how machine learning predictions throughout the entire gait cycle can enhance locomotive intent prediction among healthy individuals. Therefore, we propose a novel way of representing locomotor intent by comparing model performance during various phase windows of gait. Since prior work has not analyzed prediction performance during distinct phases of the gait cycle, this novel approach improves upon locomotor intent prediction during level-ground walking. Furthermore, the BiLSTM model has not been previously used for determining locomotor intent and is a novel architecture for this study. We hypothesized that the prediction accuracy of lower limb joint angles would be consistent across phase windows using deep learning models (LSTM and BiLSTM) but not for Random Forest. We speculate that LSTM and BiLSTM are more robust to changes in their inputs across gait phases because of their sequence learning architecture. We also hypothesized that the deep learning models would outperform traditional machine learning in overall prediction accuracy regardless of gait phase.

II. Methods

A. Participants

Thirty individuals (18 males, 12 females, age 21.97 ± 2.75 years; height 1.73±0.101 m; weight 72.92±12.57 kg) participated in the study at the Auburn University Biomechanical Engineering (AUBE) Laboratory. Exclusion criteria included lower limb injury, lower limb surgery, back injury, and back surgery within six months of testing. The protocol was approved by the Auburn University IRB (protocol no. 17-279-MR 1707), and all study participants provided written informed consent.

B. Instrumentation

A ten-camera motion capture camera system (Vicon, Oxford, U.K.) recorded marker trajectories sampled at 120 Hz, and these data were filtered using a 15 Hz Butterworth lowpass filter. Two ground-embedded force plates (AMTI, Waterford, MA, USA) at the center of the capture volume recorded gait events were sampled at 2000 Hz. As shown in Fig. 1, 79 retroreflective markers were affixed to the user using the point cluster method [37]. Fourteen EMG and 16 IMU sensors (Delsys Trigno IM, Delsys Inc., Boston, MA, USA) were attached bilaterally to the gluteus maximus, biceps femoris, vastus lateralis, gastrocnemius, tibialis anterior, erector spinae, and rectus abdominus (Fig 1). The EMG placement location was shaved and gently cleaned with isopropyl alcohol pads to remove hair and dirt on the skin surface. The sensors were then placed over the belly of the target muscle to avoid innervation zones, tendons, and crosstalk from neighboring muscles. IMUs were also attached to the dorsum of the left and right foot. IMU signals comprised of a 3-axis accelerometer (148 Hz), 3-axis gyroscope (148 Hz), and 3-axis magnetometer (74 Hz). EMG signals were sampled at 1,111 Hz and filtered using a bandpass filter of 20 Hz - 450 Hz. Motion capture trials were recorded in Vicon Nexus. Marker trajectories were synchronized with IMU signals using a MATLAB script (Mathworks, Natick, MA, United States) to align the frame number where the IMU angular velocity magnitude overlapped with the motion capture segment velocity exported from Visual3D (C-Motion, Germantown, MD, United States). EMG signals were synchronized with IMU since the Trigno IM sensors combine IMU and EMG signals within the same sensor.

C. Input and Output Variables

EMG, IMU, and joint kinematics were used as input features to the machine learning and deep learning models. The inputs comprised of 14 EMG features, 144 IMU features, and one joint kinematic feature for a total of 159 features. The joint kinematic feature used was the ankle, knee, or hip sagittal plane flexion/extension angle. Ankle angles were the only joint kinematic input feature to predict future ankle angle on the test set. Knee angle input features were used for knee angle predictions, and hip angle input features were used to predict future hip angle. The input-output model setup for predicting future joint angles was performed similarly in a previous study with EMG signals and knee flexion angle used as inputs to predict future knee flexion angle [9].

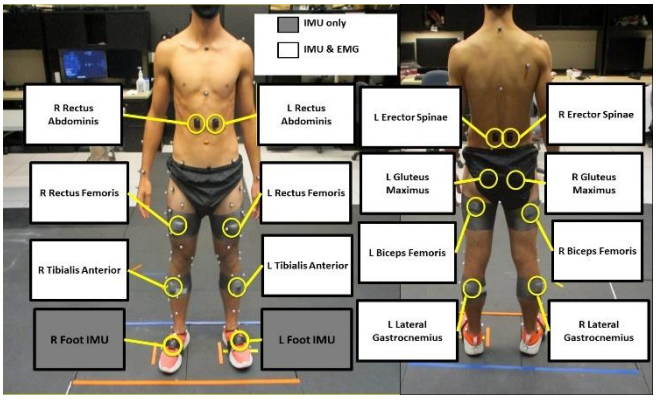

Fig. 1. Anterior and posterior views of the participant for the experimental setup. Retroreflective markers trajectories were captured to obtain user kinematics using Visual3D. Each Trigno IM Sensor contains IMU and EMG signals, while only IMU signals were used for the left and right foot.

D. Experimental Protocol

The experimental protocol is summarized in Fig. 2. The participants performed three overground walking trials along a 5-meter walkway in the lab at a self-selected pace. A successful trial occurred when the participant made heel contact on the first force plate, followed by heel contact by the contralateral limb onto the second force plate. Participants were asked to re-do the trial if this criterion was not successfully achieved to capture at least one gait cycle. Joint kinematics were processed using Visual3D to extract joint angles following the Grood & Suntay method [38].

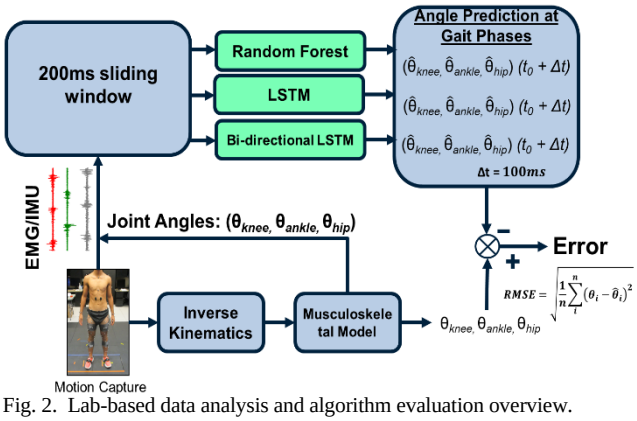

Fig. 2. Lab-based data analysis and algorithm evaluation overview.

E. Gait Phase Partitioning

The timing of heel strike and toe-off events were obtained using a built-in pipeline in Visual3D and exported for processing a full stride of the gait cycle (Fig. 3). A gait cycle was defined as beginning and ending at the heel strike of the ipsilateral limb. Gait phases used for evaluation comprised of post heel strike (PostHS), pre toe-off (PreTO), post toe-off (PostTO), and pre heel strike (PreHS). The boundary conditions were consistent with Huang et al., 2009 for classifying locomotion modes using EMG combined with several pattern recognition algorithms [14]. However, Huang et al., 2009 used 200 ms window lengths for each phase resulting in a data overlap between PostTO and PreHS during level-ground walking tasks. To avoid data overlapping, we evaluated the gait phase windows at ±15% of the gait cycle. Also, this region is within a reasonable time window of muscle action following EMG signals. Furthermore, the phase windows chosen are practical for supplying torque-based assistance that matches the user's desired intent during key points of the gait cycle. For example, plantarflexion assistance of 0.4 W/kg at 42% of the gait cycle was shown to reduce the metabolic cost of walking by 12% compared to walking without an exoskeleton [39].

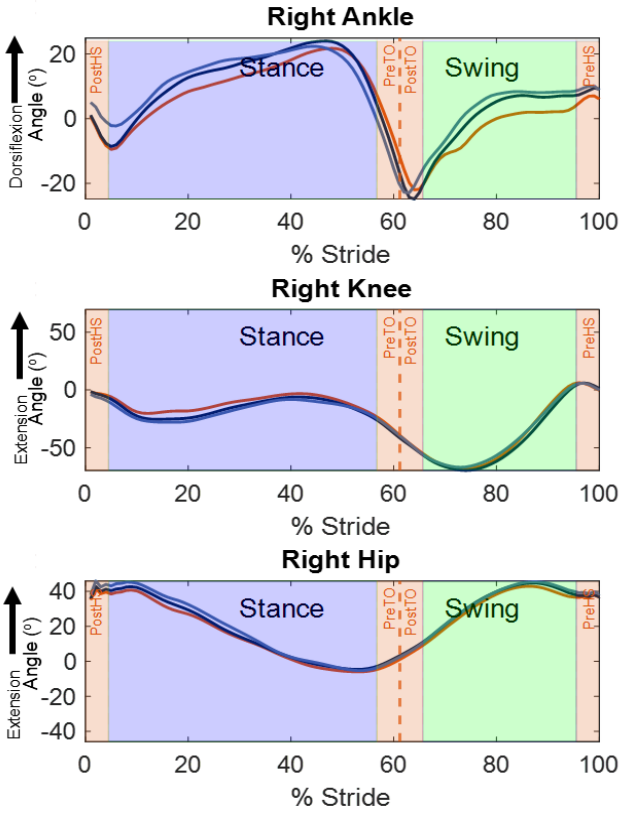

Fig. 3. Gait phases were partitioned into distinct boundary conditions. The gait cycle started and ended at the heel strike of the ipsilateral limb. This study evaluated the performance of prediction algorithms in the orange regions: post heel strike (PostHS), pre toe-off (PreTO), post toe-off (PostTO), and pre-heel strike (PreHS).

F. Data Preprocessing

Feature standardization is common in machine learning since input features with larger unit scales may dominate model performance. Standardized feature inputs tend to yield better model performance when training on neural networks [40]. EMG and IMU signals used for predicting joint angles were standardized using Python's StandardScaler preprocessing library to equalize the importance of each feature input. Following standardization, the signals were transformed as seen in (1), where *x* is the original signal, *u* is the mean of the feature column, and *s* is the standard deviation of the feature column. The mean and standard deviation from the standard scaler is then used for transforming the feature columns.

$$z = (x - u) / s \quad (1)$$

Data from Visual3D were exported and the frequency for joint angles were upsampled to 2160 Hz. EMG and IMU signal frequency was also increased to 2160 Hz to ensure the same input and output mapping was applied. This frequency was chosen to allow the models to learn a function based on the same input-output mapping dimensions, where one instance of EMG and IMU data point corresponded to a single instance of joint angle.

G. Train and Test Split

Training was randomly assigned to one walking trial and tested on another randomly selected walking trial of the same subject. This model is, therefore, considered a subject-dependent predictor. Similar to Farrell & Herr, 2011, we used a 200 ms sliding window of the input features signals with increments of 20 ms for model predictions of future joint angles 100 ms later [33]. The window length was also similar in scale to a sliding window of 150 ms and window increments of 50 ms for continuous locomotion mode prediction for volitional control of a transfemoral prosthesis [26]. Classifying locomotion mode can afford larger window sizes compared to joint-level prediction because a particular task requires larger input signals to recognize a completed task. For example, Kazemimoghadam & Fey, 2021 used a 300 ms rolling window for feature extraction with 25 ms increments to classify anticipated and unanticipated tasks of crossover cut, sidestep cut, sidestep cut to stairs, and crossover cut to stairs [7]. Kang et al., 2022 explored input window sizes between 300 ms and 1000 ms for a continuous locomotion mode classifier and found an optimal input window size of 500 ms for the deep convolutional neural network (CNN) [15]. Huang et al. tested a variety of window size increments between 10-60 ms on locomotion classification accuracy and reported the best performance using 20 ms increments [14]. Although the window size may contribute to delay due to computation in real-time systems, Kazemimoghadam & Fey, 2021 tested windows sizes between 100 and 600 ms. A 200 ms delay could result in a malfunction as 300 ms delay is considered unacceptable for real-time system [34]. However, the 200 ms input window will not result in a 200 ms delay in the system as prior studies have shown a window size of 200 ms or less to be successful for real-time applications [26], [33]. Therefore, we chose an input window size of 200 ms with 20 ms increments to increase the sensitivity because joint kinematics depend more on recent kinematics compared to activity classification. A window size of 200 ms was chosen to include enough data samples in case signal drop occurred due to communication or sensor error. The joint angles evaluated during prediction were ankle, knee, and hip angles in the sagittal plane (flexion/extension angles). In summary, the input features used for this study were EMG, IMU, and joint angles. The input features were mapped to the target labels, which were joint angles 100 ms into the future.

H. Prediction Algorithms

Joint angle prediction is considered a nonlinear sequence-to-sequence problem where a sequence of input signals from EMG and IMU is used to predict the following sequence of joint angles [25], [41]. We used a 200 ms sliding window of inputs signals to predict lower-limb joint angles at 100ms into the future. The scikit-learn machine learning library was implemented for importing a standard Random Forest Regression with default hyperparameters for prediction algorithms. TensorFlow, supported by Keras application programming Interface (API), was used to build, train, and test the two deep learning models: Long short-term memory and bidirectional long short-term memory

Random Forest Regression- Random forest has shown promise for time-series forecasting predictions in biomechanics [42], [43]. Random forest is an ensemble of decision trees that uses observations and predictor variables. Random forest was chosen because it is considered a simple yet powerful model in machine learning [16].

Long Short-Term Memory (LSTM)- A deep learning method was chosen due to its ability to perform predictions without requiring manual feature extraction [16]. The first deep learning model used was Long Short-Term Memory (LSTM), a type of recurrent neural network (RNN). The advantage of RNNs is their ability to learn temporal dependencies and contextual information of the input features, which is suitable for solving time series forecasting problems. Although standard RNNs use loops of neurons compared to feedforward networks, their main limitations are seen when their weights become so small as to have no effect (vanishing gradients) or increase exponentially and diverge (exploding gradients). LSTM is a deep learning method that overcomes the vanishing and exploding gradient problem in standard RNNs. The LSTM memory cell's internal architecture consists of a forget, input, and output gate. The memory cell enables constant data flow, called *constant error carrousel* for stability, thus allowing LSTM models to overcome the vanishing and exploding gradient problem.

Bidirectional LSTM – Bidirectional LSTMs (BiLSTM) includes an additional layer of information compared to unidirectional LSTMs. In addition to forward information flow, as seen in unidirectional LSTMs, BiLSTM includes data flow in the backward direction. Therefore, BiLSTM includes an additional LSTM layer for the backward sequence to eliminate sequence dependence in a single direction. Since past data is used to predict future joint angles, the BiLSTM uses the input sequence as-is for one LSTM layer and a reversed copy of the input sequence for the second LSTM layer. As a result, the temporal dependencies are not reliant on a single direction. Although BiLSTM has shown to be beneficial for applications in natural language processing, few studies have incorporated BiLSTM for biomechanics applications. Tan et al., 2022 used a BiLSTM to predict knee angles for individuals with knee osteoarthritis using four IMUs attached bilaterally to the thigh and shank [24]. Furthermore, the authors recommended comparing BiLSTM with traditional LSTM for kinematic predictions.

Several regularization techniques were employed to reduce overfitting of the training data for the deep learning models. The first regularization strategy was dropout for the two dense layers to prevent over-dependence on the feature inputs (Table I) [44]. The dropout probability was set to 0.5 in both dense layers [45]. Early stopping was the second regularization technique we used to improve model generalization and avoid overfitting. Early stopping prevents model overfit by ending training when improvement in the loss plateaus. Similar to Kang et al., 2020, model training was set to 200 epochs to prevent overfitting [8]. Training was stopped early when the loss function did not improve during five consecutive training epochs (i.e., we set the patience parameter for the TensorFlow callback equal to 5). The Adam optimizer was implemented during training to minimize the mean absolute error (MAE) loss function during gradient descent [8], [46]. The model architecture for the LSTM and BiLSTM used are shown in Table I. Tan et al., 2022 recommended comparing the effect of unidirectional vs. bidirectional architecture of LSTM so we chose a similar number of neurons and hidden layers for LSTM and BiLSTM [24]. In this study, unidirectional and bidirectional refers to the flow of data in the deep learning model. We chose 159 neurons for the input layer to match the input size of $\mathbb{R}^{159}$ from 16 EMG and 14 IMU sensors (14 Gyro, 14 Acc, and 14 Mag along x, y, and z-axes), and one joint angle. We performed preliminary searchers of hyperparameters based on Molinaro et al., 2022 and pilot tested 2, 3, and 4 hidden layers and dropout probabilities of 0.1, 0.3, and 0.5 [16]. After evaluating the results of the pilot testing, the LSTM architecture shown in Table I achieved the highest level of performance. Although increasing the number of neurons may increase complexity resulting in overfitting to the training data, the dropout layer probability of 0.5 reduces the amount of overfit [45]. Decreasing the dropout probability to values less than 0.5 would likely increase model complexity and overfit because more neurons are preserved at each layer during training [47]. Conversely, increasing dropout probabilities would result in a sparser network and likely result in underfitting. Two hidden layers were also chosen based on the LSTM architecture from [16].

TABLE I
Algorithm architecture for LSTM and BiLSTM

Layer Num.	Layer Type	LSTM	BiLSTM
1	LSTM Layer	LSTM of 159neurons (ReLU activation)	BiLSTM of 159 neurons
2	Dense Layer	100 neurons (ReLU activation)	100 neurons (ReLU activation)
3	Dropout Layer	0.5	0.5
4	Dense Layer	100 neurons (ReLU activation)	100 neurons (ReLU activation)
5	Dropout Layer	0.5	0.5
6	Dense Layer	1 neuron	1 neuron

I. Outcome Measures

The outcome metric to evaluate model performance was the root mean squared error (RMSE) for ankle, knee, and hip angles in the sagittal plane (2). We chose to evaluate these lower limb joint angles because they exhibit a high range of motion in the sagittal direction during walking. RMSE was chosen because it penalizes outliers more heavily than mean absolute error (MAE).

$$RMSE = \sqrt{\frac{\sum_{i=1}^{N} (x_i - \hat{x}_i)^2}{N}} \quad (2)$$

J. Statistical Analysis

We compared the performance of each algorithm for each of the four selected gait phases using Analysis of Variance (ANOVA). The initial ANOVA tested the null hypothesis that the RMSE during various phases of gait were not statistically significantly different from one another. An alpha value of 0.05 was used to assess statistical significance. Post-hoc paired t-tests with Bonferonni corrections were performed when ANOVA tests were significant. The *t*-tests performed were pair-wise comparisons for each phase

window (PostHS, PreTO, PostTO, and PreHS) for a total of six comparisons per joint.

III. Results

The model loss during training for LSTM and BiLSTM is shown in Fig. 4. The shape of the loss curves is useful to observe how well the model fits to the training data. We plotted the loss curves during training to show how early stopping effected the number of epochs during training. The loss curve shows a good fit because the loss decreased to a point of stability [48]. Although we did not report the loss function on a validation set, the RMSE on the test set was similar to a prior study using LSTM to predict lower limb kinematics during gait [25]. This suggests that the loss curves resulted in a good fit during training (Fig. 4). The test trial results for 30 subjects were evaluated using RMSE for Random Forest, LSTM, and BiLSTM (Figs. 5-7).

Overall, ankle angle predictions during PostHS, PreTO, PostTO, and PreHS ranged between a mean RMSE of 4.48-5.39 degrees for Random Forest, 2.04-3.89 degrees for LSTM, and 1.42-2.20 degrees for BiLSTM (Table II). The mean prediction RMSE at the knee during the four phase windows of gait ranged between 5.37-10.93 degrees for Random Forest, 4.27-6.59 degrees for LSTM, and 3.40-5.49 degrees for BiLSTM. Finally, the mean prediction RMSE at the hip during the four phase windows of gait ranged between 4.17-6.03 degrees for Random Forest, 3.79-5.66 degrees for LSTM, and 3.81-4.77 degrees for BiLSTM. Prediction performance for the ankle was better than the knee and hip regardless of the model used.

The one-way ANOVA resulted in a statistically significant difference in phases windows on knee angle prediction accuracy for Random Forest ($F(119, 3)=6.613$, $p<0.01$) (Table II). Significant ANOVA tests prompted Bonferroni-corrected post hoc paired *t*-tests on the gait phases for Random Forest at the knee and LSTM at the ankle. Group ANOVA comparisons that did not yield significant effects were not used for post-hoc *t*-tests. Significant *t*-tests ($p<0.05$) are shown in Table III. Random Forest had significant differences for predicting knee angle as indicated by the mean±standard deviation of the RMSE during PostHS vs. PreTO (RMSE of 5.37±3.36 deg vs. 10.93±4.70 deg), PostHS vs. PostTO (RMSE of 5.37±3.36 deg vs. 9.72±6.23 deg), and PostHS vs. PreHS (RMSE of 5.36±3.36 deg vs. 9.23±5.72 deg) (Table IV).

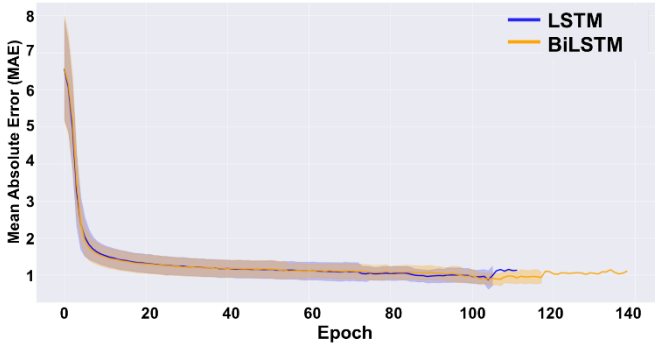

Fig 4. Model loss during training for LSTM and BiLSTM. The dark lines represent the average training loss, and the transparent regions represent one standard deviation above and below the average loss. The original training epochs were set to 200 training epochs, but early stopping with a patience of five epochs was used to prevent overfitting.

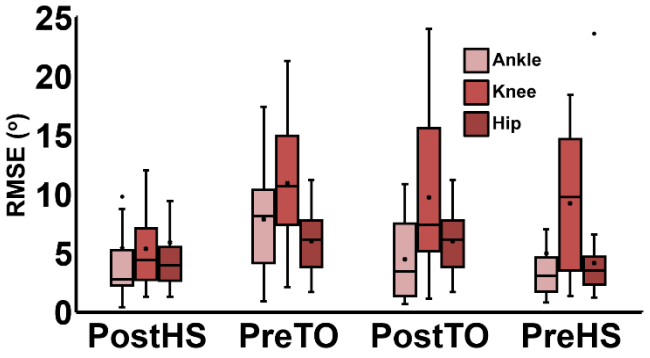

Fig. 5. Random Forest Regression results for each phase window

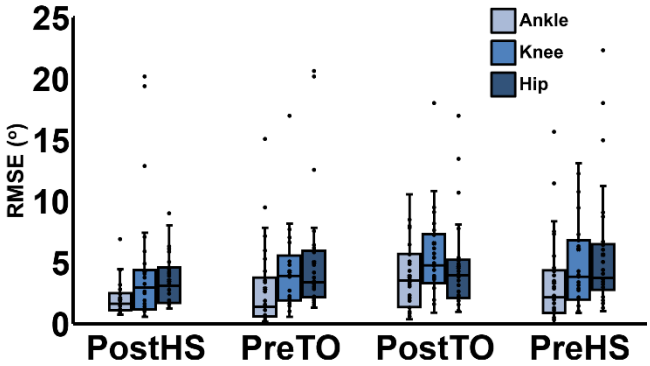

Fig. 6. LSTM results for each phase window

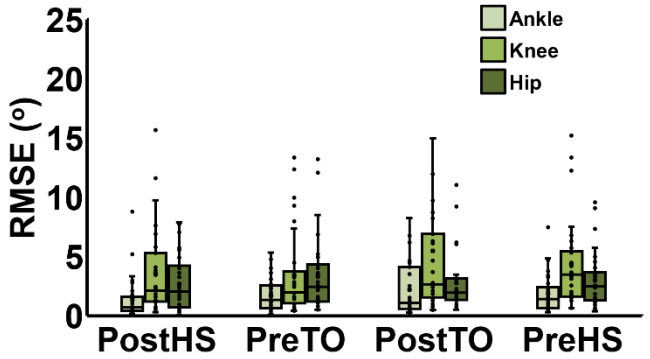

Fig. 7. Bidirectional LSTM results for each phase window

This article has been accepted for publication in IEEE Transactions on Medical Robotics and Bionics. This is the author's version which has not been fully edited and content may change prior to final publication. Citation information: DOI 10.1109/TMRB.2023.3260261

TABLE II:
The one-way ANOVA was performed to compare the effect of phase window on joint angle prediction accuracy (RMSE). ANOVA results for the random forest, LSTM, and BiLSTM are shown below. Bold values indicate statistically significant difference ($p<0.05$)

	Random Forest			**LSTM**			**BiLSTM**		
Condition	**Ankle**	**Knee**	**Hip**	**Ankle**	**Knee**	**Hip**	**Ankle**	**Knee**	**Hip**
Total df	119	119	119	119	119	119	119	119	119
F-value	1.271	6.613	0.715	2.205	0.994	1.411	0.992	1.018	0.406
p-value	0.288	**< 0.01**	0.545	0.0912	0.382	0.243	0.399	0.387	0.749
eta sq.	0.0318	0.146	0.0182	0.0540	0.0251	0.0352	0.0250	0.0257	0.0104

TABLE III
Results of post-hoc paired t-test between gait phase condition for Random Forest-Knee as it was the only condition and joint with significant ANOVA results (Table II). The results presented are Bonferroni corrected. Bold text indicates significant differences.

PostHS vs. PreTO	**PostHS vs. PostTO**	**PostHS vs. PreHS**	**PreTO vs. PostTO**	**PreTO vs. PreHS**	**PostTO vs. PreHS**
< 0.01	**0.027563**	**0.00232**	1.33724	0.558087	2.34729

TABLE IV:
Joint angle predictions performance for various phase windows reported as the mean RMSE ± one standard deviation

	Random Forest				**LSTM**				**BiLSTM**			
RMSE	**PostHS**	**PreTO**	**PostTO**	**PreHS**	**PostHS**	**PreTO**	**PostTO**	**PreHS**	**PostHS**	**PreTO**	**PostTO**	**PreHS**
Ankle	5.39±9.40	7.87±4.25	4.48±3.42	4.97±9.80	2.04±1.33	2.87±3.41	3.89±2.67	3.37±3.60	1.42±1.88	1.75±1.37	2.20±2.20	1.87±1.64
Knee	5.37±3.36	10.93±4.70	9.72±6.23	9.23±5.72	4.30±4.96	4.27±3.33	6.59±7.66	6.09±8.95	3.56±3.65	3.40±3.65	5.49±8.28	4.37±3.62
Hip	5.90±9.68	6.03±2.45	5.38±2.36	4.17±3.93	3.54±2.07	5.02±4.82	4.60±3.68	5.64±5.04	2.69±2.32	3.36±3.17	2.76±2.53	3.00±2.38

IV. Discussion

This study presented three machine learning models to predict lower limb joint angles 100 ms into the future during walking. We hypothesized that the prediction accuracy of lower limb joint angles would be consistent across phase windows using deep learning models (LSTM and BiLSTM) but not for Random Forest. ANOVA tests suggest that this hypothesis held, with statistically significant differences across phase windows observed for the Random Forest model but not for LSTM or BiLSTM when predicting knee angles. More specifically, during post-hoc *t*-tests, the Random Forest Regressor was significantly worse at predicting the knee angle during PreTO, PostTO, and PreHS than PostHS. The decrease in predictive power may have occurred because the simpler Random Forest model could not capture the complex changes occurring at the knee throughout the gait cycle. The knee involves biarticular muscles, such as the rectus femoris, which transfers energy from one joint to another [49]. EMG feature inputs of biarticular muscles connected to the knee, such as rectus femoris, biceps femoris, vastus lateralis, and gastrocnemius, may introduce additional complexity beyond what the Random Forest could handle for predicting knee angles compared to EMG of uniarticular muscles, such as the gluteus maximus, for hip angle predictions [49].

Our second hypothesis was that the deep learning methods (LSTM and BiLSTM) would outperform traditional machine learning (Random Forest), and it was also supported. Moreover, the BiLSTM prediction RMSE for this study is less than previously reported during the stance and swing phase [24]. Tan et al., 2022 used BiLSTM to predict knee angles and reported RMSE of 9.70 deg and 7.04 deg during the swing and stance phases for a single leg prediction model and 9.81 deg and 8.19 deg during swing and stance phases for a double leg prediction model [24]. Although our prediction results were reported for a subset of stance and swing phases, our knee angle predictions resulted in less overall RMSE for the phase windows occurring at the stance phase (PostHS and PreTO mean RMSE of 3.56±3.65 and 3.40±3.65 deg) and swing phase (PostTO and PreHS mean RMSE of 5.49±8.28 and 4.37±3.62 deg) (Table IV).

There are several key takeaways from this study. First, the Random Forest algorithm was worse at predicting ankle, knee, and hip angles regardless of gait phase compared to LSTM and BiLSTM. This result may suggest that deep learning algorithms may be the preferred choice for accurately predicting joint angles. However, further studies are needed to support this finding. Additionally, Random Forest predictions for knee angle were statistically significantly different across the gait cycle, which may be important when deploying a knee exoskeleton with reliable control. In the case of a knee exoskeleton, the LSTM or BiLSTM would be the preferred choice over Random Forest

based on our results. Low ankle RMSE during PreTO is desirable for an ankle exoskeleton because assistive torque during push-off phase has shown benefit among users [39], [50], [51]. Therefore, BiLSTM may be more suitable for controlling a powered ankle exoskeleton because it performed best during PreTO phase. BiLSTM also performed the best at predicting ankle angles regardless of gait phase and did not have any significant differences between the gait phases (Table II).

Overall, this study's deep learning models (LSTM and BiLSTM) performed more accurately than traditional machine learning models (Random Forest) (Table IV). Additionally, BiLSTM and LSTM were more robust to the changes in the gait phase compared to Random Forest because there were no significant differences in prediction RMSE across phase windows for LSTM and BiLSTM (Table II). Due to the additional LSTM layer processing sequence data in the inverse direction, BiLSTM is capable of contextualizing feature signals for future predictions. The BiLSTM prediction results demonstrate how specific deep learning architecture, such as an additional LSTM layer in the reverse direction, may improve prediction performance. However, there is a tradeoff between accuracy and complexity when choosing between BiLSTM vs. LSTM. Since BiLSTM has an additional LSTM layer in the reverse direction but also improves accuracy to 1.69 deg RMSE during PostTO at the ankle, consideration should be had to determine if this lift in accuracy is worth adding model complexity. Nevertheless, deep learning may be more suitable for processing continuous input streams than the Random Forest algorithm [28].

There are several applications worth noting from the results of this study. First, the results provide useful information for deploying accurate and reliable deep learning models which may be beneficial to device controllers for augmenting human movement (Table IV). Our study shows how prediction accuracy can have significantly different prediction outcomes at various phases of gait. For example, Random Forest knee predictor performed significantly better during PostHS (RMSE of 5.37±3.36 deg) compared to PreTO (RMSE of 10.93±4.70), PostTO (RMSE of 9.72±6.23 deg), and PreHS (RMSE of 9.23±5.72). This begs the question of whether it is sufficient to avoid reporting joint angle accuracies at critical phases of the gait cycle since prediction performance at certain phase windows. From the results of this study, we argue the importance of reporting prediction accuracy across various gait phases. Evaluating a model's performance using a single metric for an entire walking trial does not tell the whole story. Since performance can modulate throughout the gait cycle, as seen with the Random Forest when predicting knee angles, it is essential to select models that are both accurate and reliable.

Modifications to the model architecture in Table I may improve results for future studies on predicting locomotor intent at various speeds and slopes. For example, including more neurons and hidden layers would increase computational complexity resulting in overfitting to the training set. This would mean that the model may not generalize to unseen speeds, slopes, or individuals. Reducing the number of layers and the number of neurons per layer would likely result in a model that underfits the data. An underfitted model would have more difficulty generalizing to more complex scenarios of locomotion modes (e.g. walk-to-run and walking while turning) [7]. However, future work will perform hyperparameter tuning to optimize model architecture for locomotion modes with greater task complexity.

There are some limitations of this study worth mentioning. First, only healthy young adults participated in the study. Although the objective of this study was to predict locomotor intent among healthy individuals, the algorithms tested were limited to this population. Therefore, movement intent predictors for a different target population (e.g. individuals with musculoskeletal injury, stroke survivors, and amputees) would require further testing. The second limitation relates to the feature signals used as model inputs. The features used to train the models were EMG, IMU, and joint angles to predict joint angles 100 ms in the future. Motion capture-derived joint angles will not always be available. However, these can be measured more directly by an encoder or potentiometer, commonly found on wearable robotic systems. Lastly, this offline analysis was performed post hoc and not in real-time. Although joint angle predictions were made 100 ms into the future, a real-time machine learning-based exoskeleton may not realize a user's intent if the inherent sensor delays and model complexity within the system exceeds 30-100 ms [6], [52]. However, we intend to leverage the key points learned from the offline analysis to prepare for the online deployment of a wearable exoskeleton by incorporating deep learning models, which may be more robust. Furthermore, our results establish a foundation for real-time human motion estimation and exoskeleton control. In this study, we instructed participants to walk at a normal self-selected speed. Although we did not control for walking speed, the study participants walked with a speed of (mean ± standard deviation) 1.26 ± 0.15 m/s, which is within a reasonable range for healthy walking speed [53].

Future work to improve the study's outcomes includes tuning model hyperparameters to improve prediction performance. Since our study used 14 IMU, 16 EMG sensors, and joint angles as input features, performing dimensionality reduction could improve performance and computational efficiency. Additionally, down-selecting input features using dimensionality reduction may indicate that fewer sensors are needed for predicting each gait phase [54]. This study used subject-dependent predictors for locomotor intent. Future work will leverage deep learning models trained on large and diverse datasets for a subject-independent predictor. Also, adapting assistive devices to users based on visual feedback to enhance a user's sense of agency is worth exploring [55]. Moreover, personalized feedback may lead to subject-independent models where users accelerate the processing of co-adapting to the assistive device [51].

V. Conclusion

Our results demonstrate how improving deep learning architecture can lead to more robust human motion prediction compared to a traditional machine learning approach. Overall, the BiLSTM produced the best results and maintained consistent prediction accuracies of lower limb joint angles throughout the gait cycle. Therefore, deep learning methods, such as BiLSTM, may be preferred for controlling an ankle exoskeleton during walking since they are better suited to predict critical phases of gait, such as pre-toe-off.

Acknowledgment

We thank the U.S. Army Combat Capabilities Development Command (CCDC) for funding this study (W15QKN-17-9-1025-RPP-10 MOB 17-08?).

References

[1] "Products - Data Briefs - Number 443 - August 2022," Aug. 29, 2022. https://www.cdc.gov/nchs/products/databriefs/db443.htm (accessed Jan. 20, 2023).

[2] J. D. Omura, E. N. Ussery, F. Loustalot, J. E. Fulton, and S. A. Carlson, "Walking as an Opportunity for Cardiovascular Disease Prevention," *Prev. Chronic. Dis.*, vol. 16, p. E66, May 2019, doi: 10.5888/pcd16.180690.

[3] P. Slade, M. J. Kochenderfer, S. L. Delp, and S. H. Collins, "Personalizing exoskeleton assistance while walking in the real world," *Nature*, vol. 610, no. 7931, Art. no. 7931, Oct. 2022, doi: 10.1038/s41586-022-05191-1.

[4] A. J. Young and D. P. Ferris, "State of the Art and Future Directions for Lower Limb Robotic Exoskeletons," *IEEE Trans. Neural Syst. Rehabil. Eng.*, vol. 25, no. 2, pp. 171–182, Feb. 2017, doi: 10.1109/TNSRE.2016.2521160.

[5] K. Mudie, D. Billing, A. Garofolini, T. Karakolis, and M. LaFiandra, "The need for a paradigm shift in the development of military exoskeletons," *Eur. J. Sport Sci.*, vol. 22, no. 1, pp. 35–42, Jan. 2022, doi: 10.1080/17461391.2021.1923813.

[6] M. R. Tucker *et al.*, "Control strategies for active lower extremity prosthetics and orthotics: a review," *J. NeuroEngineering Rehabil.*, vol. 12, no. 1, p. 1, Jan. 2015, doi: 10.1186/1743-0003-12-1.

[7] M. Kazemimoghadam and N. P. Fey, "Continuous Classification of Locomotion in Response to Task Complexity and Anticipatory State," *Front. Bioeng. Biotechnol.*, vol. 9, 2021, Accessed: Jun. 07, 2022. [Online]. Available: https://www.frontiersin.org/article/10.3389/fbioe.2021.628050

[8] I. Kang, P. Kunapuli, and A. J. Young, "Real-Time Neural Network-Based Gait Phase Estimation Using a Robotic Hip Exoskeleton," *IEEE Trans. Med. Robot. Bionics*, vol. 2, no. 1, pp. 28–37, Feb. 2020, doi: 10.1109/TMRB.2019.2961749.

[9] J. Coker, H. Chen, M. C. Schall, S. Gallagher, and M. Zabala, "EMG and Joint Angle-Based Machine Learning to Predict Future Joint Angles at the Knee," *Sensors*, vol. 21, no. 11, Art. no. 11, Jan. 2021, doi: 10.3390/s21113622.

[10] J. Conte Alcaraz, S. Moghaddamnia, and J. Peissig, "Efficiency of deep neural networks for joint angle modeling in digital gait assessment," *EURASIP J. Adv. Signal Process.*, vol. 2021, no. 1, p. 10, Dec. 2021, doi: 10.1186/s13634-020-00715-1.

[11] A. T. M. Willemsen, F. Bloemhof, and H. B. K. Boom, "Automatic stance-swing phase detection from accelerometer data for peroneal nerve stimulation," *IEEE Trans. Biomed. Eng.*, vol. 37, no. 12, pp. 1201–1208, Dec. 1990, doi: 10.1109/10.64463.

[12] S. K. Ng and H. J. Chizeck, "Fuzzy model identification for classification of gait events in paraplegics," *IEEE Trans. Fuzzy Syst.*, vol. 5, no. 4, pp. 536–544, Nov. 1997, doi: 10.1109/91.649904.

[13] H. Huang, F. Zhang, L. J. Hargrove, Z. Dou, D. R. Rogers, and K. B. Englehart, "Continuous Locomotion-Mode Identification for Prosthetic Legs Based on Neuromuscular–Mechanical Fusion," *IEEE Trans. Biomed. Eng.*, vol. 58, no. 10, pp. 2867–2875, Oct. 2011, doi: 10.1109/TBME.2011.2161671.

[14] H. Huang $^\\ast$, T. A. Kuiken, and R. D. Lipschutz, "A Strategy for Identifying Locomotion Modes Using Surface Electromyography," *IEEE Trans. Biomed. Eng.*, vol. 56, no. 1, pp. 65–73, Jan. 2009, doi: 10.1109/TBME.2008.2003293.

[15] I. Kang, D. Molinaro, G. Choi, J. Camargo, and A. Young, "Subject-Independent Continuous Locomotion Mode Classification for Robotic Hip Exoskeleton Applications," *IEEE Trans. Biomed. Eng.*, pp. 1–1, 2022, doi: 10.1109/TBME.2022.3165547.

[16] D. D. Molinaro, I. Kang, J. Camargo, M. C. Gombolay, and A. J. Young, "Subject-Independent, Biological Hip Moment Estimation During Multimodal Overground Ambulation Using Deep Learning," *IEEE Trans. Med. Robot. Bionics*, vol. 4, no. 1, pp. 219–229, Feb. 2022, doi: 10.1109/TMRB.2022.3144025.

[17] J. Camargo, D. Molinaro, and A. Young, "Predicting biological joint moment during multiple ambulation tasks," *J. Biomech.*, vol. 134, p. 111020, Mar. 2022, doi: 10.1016/j.jbiomech.2022.111020.

[18] M. K. Shepherd and E. J. Rouse, "Design and Validation of a Torque-Controllable Knee Exoskeleton for Sit-to-Stand Assistance," *IEEEASME Trans. Mechatron.*, vol. 22, no. 4, pp. 1695–1704, Aug. 2017, doi: 10.1109/TMECH.2017.2704521.

[19] K. G. Gruben and W. L. Boehm, "Ankle torque control that shifts the center of pressure from heel to toe contributes non-zero sagittal plane angular momentum during human walking," *J. Biomech.*, vol. 47, no. 6, pp. 1389–1394, Apr. 2014, doi: 10.1016/j.jbiomech.2014.01.034.

[20] W. Wang, J. Chen, J. Ding, J. Zhang, and J. Liu, "Improving Walking Economy With an Ankle Exoskeleton Prior to Human-in-the-Loop Optimization," *Front. Neurorobotics*, vol. 15, p. 797147, Jan. 2022, doi: 10.3389/fnbot.2021.797147.

[21] W. Wu, K. R. Saul, and H. (Helen) Huang, "Using Reinforcement Learning to Estimate Human Joint Moments From Electromyography or Joint Kinematics: An Alternative Solution to Musculoskeletal-Based

Biomechanics," *J. Biomech. Eng.*, vol. 143, no. 4, Feb. 2021, doi: 10.1115/1.4049333.

[22] L. Rose, M. C. F. Bazzocchi, and G. Nejat, "End-to-End Deep Reinforcement Learning for Exoskeleton Control," in *2020 IEEE International Conference on Systems, Man, and Cybernetics (SMC)*, Oct. 2020, pp. 4294–4301. doi: 10.1109/SMC42975.2020.9283306.

[23] V. Lajeunesse, C. Vincent, F. Routhier, E. Careau, and F. Michaud, "Exoskeletons' design and usefulness evidence according to a systematic review of lower limb exoskeletons used for functional mobility by people with spinal cord injury," *Disabil. Rehabil. Assist. Technol.*, vol. 11, no. 7, pp. 535–547, Oct. 2016, doi: 10.3109/17483107.2015.1080766.

[24] J.-S. Tan *et al.*, "Predicting Knee Joint Kinematics from Wearable Sensor Data in People with Knee Osteoarthritis and Clinical Considerations for Future Machine Learning Models," *Sensors*, vol. 22, no. 2, p. 446, Jan. 2022, doi: 10.3390/s22020446.

[25] M. Mundt *et al.*, "Prediction of lower limb joint angles and moments during gait using artificial neural networks," *Med. Biol. Eng. Comput.*, vol. 58, no. 1, pp. 211–225, Jan. 2020, doi: 10.1007/s11517-019-02061-3.

[26] F. Zhang and H. Huang, "Source Selection for Real-time User Intent Recognition towards Volitional Control of Artificial Legs," *IEEE J. Biomed. Health Inform.*, vol. 17, no. 5, p. 907, Sep. 2013, doi: 10.1109/JBHI.2012.2236563.

[27] O. Kannape and H. Herr, "Volitional control of ankle plantar flexion in a powered transtibial prosthesis during stair-ambulation," *2014 36th Annu. Int. Conf. IEEE Eng. Med. Biol. Soc. EMBC 2014*, vol. 2014, pp. 1662–5, Aug. 2014, doi: 10.1109/EMBC.2014.6943925.

[28] F. A. Gers, D. Eck, and J. Schmidhuber, "Applying LSTM to Time Series Predictable through Time-Window Approaches," in *Artificial Neural Networks — ICANN 2001*, Berlin, Heidelberg, 2001, pp. 669–676. doi: 10.1007/3-540-44668-0_93.

[29] M. Q *et al.*, "Flexible lower limb exoskeleton systems: A review," *NeuroRehabilitation*, Feb. 2022, doi: 10.3233/NRE-210300.

[30] I. Sutskever, O. Vinyals, and Q. V. Le, "Sequence to Sequence Learning with Neural Networks," in *Advances in Neural Information Processing Systems*, 2014, vol. 27. Accessed: May 26, 2022. [Online]. Available: https://proceedings.neurips.cc/paper/2014/hash/a14ac55a4f27472c5d894ec1c3c743d2-Abstract.html

[31] T. Teramae, T. Noda, and J. Morimoto, "EMG-Based Model Predictive Control for Physical Human–Robot Interaction: Application for Assist-As-Needed Control," *IEEE Robot. Autom. Lett.*, vol. 3, no. 1, pp. 210–217, Jan. 2018, doi: 10.1109/LRA.2017.2737478.

[32] Y. Chen *et al.*, "A Continuous Estimation Model of Upper Limb Joint Angles by Using Surface Electromyography and Deep Learning Method," *IEEE Access*, vol. 7, pp. 174940–174950, 2019, doi: 10.1109/ACCESS.2019.2956951.

[33] M. T. Farrell and H. Herr, "A method to determine the optimal features for control of a powered lower-limb prostheses," in *2011 Annual International Conference of the IEEE Engineering in Medicine and Biology Society*, Aug. 2011, pp. 6041–6046. doi: 10.1109/IEMBS.2011.6091493.

[34] D. Novak and R. Riener, "A survey of sensor fusion methods in wearable robotics," *Robot. Auton. Syst.*, vol. 73, pp. 155–170, Nov. 2015, doi: 10.1016/j.robot.2014.08.012.

[35] R. D. Gurchiek, N. Cheney, and R. S. McGinnis, "Estimating Biomechanical Time-Series with Wearable Sensors: A Systematic Review of Machine Learning Techniques," *Sensors*, vol. 19, no. 23, Nov. 2019, doi: 10.3390/s19235227.

[36] H. Ma, C. Zhong, B. Chen, K.-M. Chan, and W.-H. Liao, "User-Adaptive Assistance of Assistive Knee Braces for Gait Rehabilitation," *IEEE Trans. Neural Syst. Rehabil. Eng.*, vol. 26, no. 10, pp. 1994–2005, Oct. 2018, doi: 10.1109/TNSRE.2018.2868693.

[37] T. P. Andriacchi, E. J. Alexander, M. K. Toney, C. Dyrby, and J. Sum, "A Point Cluster Method for In Vivo Motion Analysis: Applied to a Study of Knee Kinematics," *J. Biomech. Eng.*, vol. 120, no. 6, pp. 743–749, Dec. 1998, doi: 10.1115/1.2834888.

[38] E. S. Grood and W. J. Suntay, "A Joint Coordinate System for the Clinical Description of Three-Dimensional Motions: Application to the Knee," *J. Biomech. Eng.*, vol. 105, no. 2, pp. 136–144, May 1983, doi: 10.1115/1.3138397.

[39] S. Galle, P. Malcolm, S. H. Collins, and D. De Clercq, "Reducing the metabolic cost of walking with an ankle exoskeleton: interaction between actuation timing and power," *J. NeuroEngineering Rehabil.*, vol. 14, no. 1, p. 35, Dec. 2017, doi: 10.1186/s12984-017-0235-0.

[40] M. Shanker, M. Y. Hu, and M. S. Hung, "Effect of data standardization on neural network training," *Omega*, vol. 24, no. 4, pp. 385–397, Aug. 1996, doi: 10.1016/0305-0483(96)00010-2.

[41] M. Mundt *et al.*, "Estimation of Gait Mechanics Based on Simulated and Measured IMU Data Using an Artificial Neural Network," *Front. Bioeng. Biotechnol.*, vol. 8, p. 41, Feb. 2020, doi: 10.3389/fbioe.2020.00041.

[42] M. H. Schwartz, A. Rozumalski, W. Truong, and T. F. Novacheck, "Predicting the outcome of intramuscular psoas lengthening in children with cerebral palsy using preoperative gait data and the random forest algorithm," *Gait Posture*, vol. 37, no. 4, pp. 473–479, Apr. 2013, doi: 10.1016/j.gaitpost.2012.08.016.

[43] J. D. Farah, N. Baddour, and E. D. Lemaire, "Gait phase detection from thigh kinematics using machine learning techniques," in *2017 IEEE International Symposium on Medical Measurements and Applications (MeMeA)*, May 2017, pp. 263–268. doi: 10.1109/MeMeA.2017.7985886.

[44] A. Krizhevsky, I. Sutskever, and G. E. Hinton, "ImageNet Classification with Deep Convolutional Neural Networks," in *Advances in Neural Information Processing Systems*, 2012, vol. 25. Accessed: Jun. 07, 2022. [Online]. Available: https://proceedings.neurips.cc/paper/2012/hash/c399862d3b9d6b76c8436e924a68c45b-Abstract.html

[45] J. Ba and B. Frey, "Adaptive dropout for training deep neural networks," in *Advances in Neural Information Processing Systems*, 2013, vol. 26. Accessed: Jun. 06,

2022. [Online]. Available: https://proceedings.neurips.cc/paper/2013/hash/7b5b23f4aadf9513306bcd59afb6e4c9-Abstract.html

[46] D. P. Kingma and J. Ba, "Adam: A Method for Stochastic Optimization," *ArXiv14126980 Cs*, Jan. 2017, Accessed: Apr. 20, 2022. [Online]. Available: http://arxiv.org/abs/1412.6980

[47] N. Srivastava, G. Hinton, A. Krizhevsky, I. Sutskever, and R. Salakhutdinov, "Dropout: A Simple Way to Prevent Neural Networks from Overfitting".

[48] I. Goodfellow, Y. Bengio, and A. Courville, *Deep learning*. Cambridge, Massachusetts: The MIT Press, 2016.

[49] B. I. Prilutsky and V. M. Zatsiorsky, "Tendon action of two-joint muscles: Transfer of mechanical energy between joints during jumping, landing, and running," *J. Biomech.*, vol. 27, no. 1, pp. 25–34, Jan. 1994, doi: 10.1016/0021-9290(94)90029-9.

[50] G. M. Bryan, P. W. Franks, S. C. Klein, R. J. Peuchen, and S. H. Collins, "A hip–knee–ankle exoskeleton emulator for studying gait assistance," *Int. J. Robot. Res.*, p. 0278364920961452, Nov. 2020, doi: 10.1177/0278364920961452.

[51] G. M. Gasparri, J. Luque, and Z. F. Lerner, "Proportional Joint-Moment Control for Instantaneously Adaptive Ankle Exoskeleton Assistance," *IEEE Trans. Neural Syst. Rehabil. Eng.*, vol. 27, no. 4, pp. 751–759, Apr. 2019, doi: 10.1109/TNSRE.2019.2905979.

[52] P. R. Cavanagh and P. V. Komi, "Electromechanical delay in human skeletal muscle under concentric and eccentric contractions," *Eur. J. Appl. Physiol.*, vol. 42, no. 3, pp. 159–163, Nov. 1979, doi: 10.1007/BF00431022.

[53] R. W. Bohannon and A. Williams Andrews, "Normal walking speed: a descriptive meta-analysis," *Physiotherapy*, vol. 97, no. 3, pp. 182–189, Sep. 2011, doi: 10.1016/j.physio.2010.12.004.

[54] Z. Li, X. Guan, K. Zou, and C. Xu, "Estimation of Knee Movement from Surface EMG Using Random Forest with Principal Component Analysis," *Electronics*, vol. 9, no. 1, p. 43, Dec. 2019, doi: 10.3390/electronics9010043.

[55] R. Nataraj, D. Hollinger, M. Liu, and A. Shah, "Disproportionate positive feedback facilitates sense of agency and performance for a reaching movement task with a virtual hand," *PLOS ONE*, vol. 15, no. 5, p. e0233175, May 2020, doi: 10.1371/journal.pone.0233175.